

Principles of the Construction of Polymer Structures, Heteronuclear (^{13}C , ^{15}N) CP-MAS NMR, and Thermal Behavior of Heteroleptic Bismuth(III) Complexes of the General Composition $[\text{Bi}(\text{S}_2\text{CNR}_2)_2\text{X}]$ ($\text{X} = \text{NO}_3, \text{Cl}$)

E. V. Novikova^a, A. V. Ivanov^{a, *}, I. V. Egorova^b, R. S. Troshina^b, N. A. Rodionova^b,
A. I. Smolentsev^{c, d}, and O. N. Antzutkin^{e, f}

^aInstitute of Geology and Nature Management, Far East Branch, Russian Academy of Sciences, Blagoveshchensk, 675000 Russia

^bBlagoveshchensk State Pedagogical University, Blagoveshchensk, 675000 Russia

^cNikolaev Institute of Inorganic Chemistry, Siberian Branch, Russian Academy of Sciences, Novosibirsk, 630090 Russia

^dNovosibirsk State University, Novosibirsk, 630090 Russia

^eLuleå University of Technology, Luleå, Sweden

^fUniversity of Warwick, Coventry, United Kingdom

*e-mail: alexander.v.ivanov@chemist.com

Received March 29, 2019; revised April 8, 2019; accepted April 22, 2019

Abstract—The crystalline heteroleptic bismuth(III) complexes, $[\text{Bi}\{\text{S}_2\text{CN}(\text{iso-C}_4\text{H}_9)_2\}_2(\text{NO}_3)]$ (**I**) and $[\text{Bi}\{\text{S}_2\text{CN}(\text{C}_3\text{H}_7)_2\}_2\text{Cl}]$ (**II**), are isolated in preparative yields. Both compounds form 1D polymer structures and are characterized by X-ray diffraction analysis (CIF files CCDC nos. 1877115 (**I**) and 1876364 (**II**)) and (^{13}C , ^{15}N) CP-MAS NMR spectroscopy. The coordination mode of each of the dialkyldithiocarbamate ligands is S,S'-anisobidentately terminal. The inorganic anions performing the μ_2 -bridging function participate in the binding of the adjacent metallic atoms to form zigzag polymer chains. A new mode of bismuth(III) binding involving all oxygen atoms (*O,O'*-anisobidentate coordination to each adjacent bismuth atom) is found for the bridging nitrate groups in compound **I**. The bismuth atoms in the studied compounds are characterized by the eightfold $[\text{BiS}_4\text{O}_4]$ (**I**) or sixfold $[\text{BiS}_4\text{Cl}_2]$ (**II**) environment. The thermal behavior of the synthesized complexes is characterized by the data of simultaneous thermal analysis, using parallel recording of thermogravimetry and differential scanning calorimetry curves. In both cases, Bi_2S_3 is the only final product of the thermal transformations of compounds **I** and **II**.

Keywords: heteroleptic bismuth(III) complexes, dialkyldithiocarbamate ligands, 1D polymer structures, thermal behavior, X-ray diffraction analysis, heteronuclear (^{13}C , ^{15}N) MAS NMR spectroscopy

DOI: 10.1134/S1070328419100038

INTRODUCTION

The low toxicity of bismuth and its compounds compared to other heavy metals, on the one hand, predetermined a tendency in industry to replace lead and antimony by bismuth and, on the other hand, makes it possible to use the bismuth(III) complexes in the production of drugs with antiulcer, anti-inflammatory, and antibacterial activity. The bismuth complexes, including those with dialkyldithiocarbamate ligands, exhibit antibacterial [1–4] and also anticancer activity [5–9]. In addition to the dithiocarbamate complexes [2–4, 9–18], bismuth(III) also forms heteroleptic compounds, whose inner sphere contains the inorganic anions along with $=\text{NC}(\text{S})\text{S}-$ groups: NO_3^- [19–24] and X^-

($\text{X} = \text{Cl}, \text{Br}, \text{I}$) [25–28]. The latter can be used for the production of materials based on the Bi_2S_3 films and nanoparticles [24, 27].

In this work, we preparatively isolated the crystalline heteroleptic bismuth(III) complexes of the general composition $[\text{Bi}(\text{S}_2\text{CNR}_2)_2\text{X}]$ ($\text{R} = \text{iso-C}_4\text{H}_9$, $\text{X} = \text{NO}_3$ (**I**); $\text{R} = \text{C}_3\text{H}_7$, $\text{X} = \text{Cl}$ (**II**)). According to the X-ray diffraction analysis data, the complexes form 1D polymer structures. The synthesized compounds were characterized by the data of (^{13}C , ^{15}N) CP-MAS NMR spectroscopy. Their thermal behavior was studied by simultaneous thermal analysis (STA).

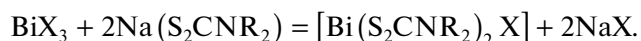
EXPERIMENTAL

The initial compounds $\text{Na}\{\text{S}_2\text{CN}(\text{C}_3\text{H}_7)_2\} \cdot \text{H}_2\text{O}$ and $\text{Na}\{\text{S}_2\text{CN}(\text{iso-C}_4\text{H}_9)_2\} \cdot 3\text{H}_2\text{O}$ were synthesized by the reactions of the corresponding dialkylamines, $\text{HN}(\text{C}_3\text{H}_7)_2$ (Merck) and $\text{HN}(\text{iso-C}_4\text{H}_9)_2$ (Aldrich), with carbon bisulfide (Merck) taken in equimolar amounts in an alkaline medium [29].

IR (KBr; ν , cm^{-1}) for $\text{Na}\{\text{S}_2\text{CN}(\text{iso-C}_4\text{H}_9)_2\} \cdot 3\text{H}_2\text{O}$: 3362 s.br, 2961 s, 2933 m, 2893 vw, 2867 m, 1641 m, 1596 m, 1477 s, 1463 w, 1424 w, 1400 m, 1382 m, 1367 w, 1355 m, 1337 w, 1290 m, 1233 s, 1202 m, 1169 w, 1150 m, 1090 s, 1009 w, 972 s, 936 m, 909 w, 868 m, 817 w, 805 w, 612 m, 557 w, 467 w; for $\text{Na}\{\text{S}_2\text{CN}(\text{C}_3\text{H}_7)_2\} \cdot \text{H}_2\text{O}$: 3368 s.br, 2963 m, 2930 m, 2872 m, 2130 s, 1632 s, 1468 s, 1408 s, 1368 s, 1304 m, 1298 m, 1267 m, 1237 s, 1198 s, 1138 s, 1107 w, 1088 m, 1028 m, 970 s, 891 m, 864 m, 745 m, 602 w, 536 w [18].

^{13}C CP-MAS NMR (δ , ppm) for $\text{Na}\{\text{S}_2\text{CN}(\text{iso-C}_4\text{H}_9)_2\} \cdot 3\text{H}_2\text{O}$: 208.2 ($-\text{S}_2\text{CN}=\text{}$); 66.7 ($=\text{NCH}_2-$); 28.0, 27.1 (1 : 1, $=\text{CH}-$); 23.0, 22.4, 20.8 (1 : 1 : 2, $-\text{CH}_3$) [30]; for $\text{Na}\{\text{S}_2\text{CN}(\text{C}_3\text{H}_7)_2\} \cdot \text{H}_2\text{O}$: 208.3 ($-\text{S}_2\text{CN}=\text{}$); 59.4, 57.9 (1 : 1, $=\text{NCH}_2-$); 22.3, 21.5 (1 : 1, $-\text{CH}_2-$); 12.6, 11.5 (1 : 1, $-\text{CH}_3$) [30].

Syntheses of the 1D polymer complexes, *catena*-poly[(μ_2 -nitrate-*O*,{*O'*,*O''*})bis(*N,N*-di-*iso*-butyldithiocarbamate-*S,S'*)bismuth(III)] (**I**) and *catena*-poly[(μ_2 -chloro)bis(*N,N*-dipropyldithiocarbamate-*S,S'*)bis-muth(III)] (**II**), were carried out via the following reaction:



For compounds **I** and **II**, the reaction between $\text{Bi}(\text{NO}_3)_3 \cdot 5\text{H}_2\text{O}$ and $\text{Na}\{\text{S}_2\text{CN}(\text{iso-C}_4\text{H}_9)_2\} \cdot 3\text{H}_2\text{O}$ / $\text{BiCl}_3 \cdot \text{H}_2\text{O}$ or $\text{Na}\{\text{S}_2\text{CN}(\text{C}_3\text{H}_7)_2\} \cdot \text{H}_2\text{O}$ was carried out in an acetone–ethanol (1 : 1) system or in an acetone solution, respectively. The starting bismuth salts were used in a 5% stoichiometric excess. The reaction mixtures were magnetically stirred for 1 h and left to stay at room temperature. Then the solutions were separated from the formed precipitates by filtration with additional washing of the target complexes from the precipitate phase with the corresponding solvents. Yellow plate-like crystals of complexes **I** or **II** were obtained by the slow evaporation of the solvents at room temperature (a minor amount CH_2Cl_2 was added to the solution to improve the crystallization of compound **I**). The yields of compounds **I** and **II** were 64.4 and 78.0%, respectively; and mp = 155–158 and 146–148°C for compounds **I** and **II**, respectively.

IR for complex **I** (KBr; ν , cm^{-1}): 2962 s, 2930 m, 2898 vw, 2871 m, 1634 m, 1501 s, 1485 m, 1466 m, 1431 s, 1385 s, 1369 vw, 1358 m, 1339 m, 1311 s, 1249 s, 1195 m, 1171 w, 1149 s, 1128 w, 1122 w, 1090 w, 1032 m, 970 m, 921 m, 885 w, 818 w, 714 w, 707 vw, 628 w, 607 w, 532 w; for complex **II**: 2964 s, 2929 m, 2870 m, 1493 s, 1464 m, 1428 s, 1363 m, 1341 w, 1303 m,

1270 w, 1241 s, 1197 m, 1148 s, 1102 w, 1087 m, 1032 w, 962 m, 894 m, 765 w, 752 m, 619 w, 602 m, 536 w.

^{13}C , ^{15}N CP-MAS NMR for complex **I** (δ , ppm): 204.4, 199.9 (1 : 1, $-\text{S}_2\text{CN}=\text{}$); 63.7, 61.9, 57.6 (1 : 1 : 2, $=\text{NCH}_2-$); 29.4, 28.2, 26.5 (1 : 1 : 2, $-\text{CH}=\text{}$); 23.6, 22.4, 21.8, 21.4, 20.8, 19.6, 19.0 (1 : 2 : 1 : 1 : 1 : 1 : 1, $-\text{CH}_3$); 146.4, 140.1 (1 : 1, $-\text{S}_2\text{CN}=\text{}$); 336.5 (NO_3^-); **II**: 200.1, 199.3 (1 : 1, $-\text{S}_2\text{CN}=\text{}$); 57.7, 56.7, 55.6 (1 : 1 : 2, $=\text{NCH}_2-$); 23.0, 20.8, 20.1 (1 : 2 : 1, $-\text{CH}_2-$); 13.2, 12.7, 11.8 (1 : 2 : 1, $-\text{CH}_3$); 143.7, 141.3 (1 : 1, $-\text{S}_2\text{CN}=\text{}$).

$^{13}\text{C}/^{15}\text{N}$ CP-MAS NMR spectra were recorded on an Ascend Aeon (Bruker) with the working frequency of 100.64/40.55 MHz a superconducting magnet ($B_0 = 9.4$ T) with the closed cycle of helium condensation through an external compressor, and the Fourier transform. Proton cross polarization (CP) was used with the contact time $^1\text{H}-^{13}\text{C}/^1\text{H}-^{15}\text{N}$ 2.0/1.5 ms. The $^{13}\text{C}-^1\text{H}/^{15}\text{N}-^1\text{H}$ interaction suppression was based on the decoupling effect using the radiofrequency field at the resonance proton frequency (400.21 MHz) [31]. Polycrystalline samples of compounds **I** (~61 mg) and **II** (~29 mg) were placed in a 4.0-mm ZrO_2 ceramic rotor. For measuring the $^{13}\text{C}/^{15}\text{N}$ NMR spectra, the rotation of the samples under the magic angle (MAS) was used at the frequency 5000–10000/5000(1) Hz, the number of acquisitions was 23400–30000/31648–78200, the duration of the proton $\pi/2$ pulses was 2.7/2.7 μs , and the interval between pulses was 2.0/2.0 s. The isotropic chemical shifts $\delta(^{13}\text{C})/\delta(^{15}\text{N})$ are given relative to one of the components of crystalline adamantane as an external standard ($\delta = 38.48$ ppm relative to tetramethylsilane)/crystalline NH_4Cl ($\delta = 0.0$ ppm, –341 ppm in the absolute scale [32]) with a correction to the drift of the magnetic field strength, the frequency equivalent of which was 0.031/0.011 Hz/h. The magnetic field homogeneity was controlled by the width (2.6 Hz) of the reference line of adamantane.

The IR spectra of complexes **I** and **II** pressed in KBr pellets were recorded on FSM–1201 and FSM–2202 interference FTIR spectrometers in ranges of 450–7500 and 400–4000 cm^{-1} . The instruments were controlled and the spectra were processed using the FSpec program (version 4.0.0.2 for Windows, OOO Monitoring, Russia).

X-ray diffraction analyses of complexes I and II were carried out from plate-like single crystals on Bruker-Nonius X8 Apex CCD and Bruker SMART 1000 CCD diffractometers at 150(2) and 120(2) K (MoK_α radiation, $\lambda = 0.71073$ Å, graphite monochromator). The data were collected using a standard procedure: φ and ω scan modes for narrow frames or in a hemisphere range. An absorption correction was applied empirically (SADABS) [33]. The structures were determined by a direct method and refined by least squares (for F^2)

Table 1. Crystallographic data and experimental structure refinement parameters for compounds [Bi{S₂CN(*iso*-C₄H₉)₂}₂(NO₃)] (**I**) and [Bi{S₂CN(C₃H₇)₂}₂Cl] (**II**)

Parameter	Value	
	I	II
Empirical formula	C ₁₈ H ₃₆ N ₃ O ₃ S ₄ Bi	C ₁₄ H ₂₈ N ₂ S ₄ ClBi
<i>FW</i>	679.72	597.05
Crystal system	Orthorhombic	Monoclinic
Space group	<i>Pca</i> 2 ₁	<i>P</i> 2 ₁ / <i>c</i>
<i>a</i> , Å	11.1947(7)	9.6492(12)
<i>b</i> , Å	10.8399(6)	24.466(3)
<i>c</i> , Å	21.5113(11)	9.2616(11)
β, deg	90	95.514(3)
<i>V</i> , Å ³	2610.4(3)	2176.4(5)
<i>Z</i>	4	4
ρ _{calc} , g/cm ³	1.730	1.822
μ, mm ⁻¹	7.097	8.606
<i>F</i> (000)	1344	1160
Crystal size, mm ³	0.25 × 0.25 × 0.06	0.25 × 0.21 × 0.10
Range of data collection over θ, deg	2.62–27.50	2.12–28.00
Ranges of reflection indices	–9 ≤ <i>h</i> ≤ 14, –14 ≤ <i>k</i> ≤ 12, –27 ≤ <i>l</i> ≤ 23	–12 ≤ <i>h</i> ≤ 12, –32 ≤ <i>k</i> ≤ 32, –12 ≤ <i>l</i> ≤ 12
Number of measured reflections	15835	20874
Number of independent reflections (<i>R</i> _{int})	5637 (0.0267)	5224 (0.0495)
Number of reflections with <i>I</i> > 2σ(<i>I</i>)	5327	5224
Number of refinement variables	271	203
GOOF	0.896	1.007
<i>R</i> factors for <i>F</i> ² > 2σ(<i>F</i> ²)	<i>R</i> ₁ = 0.0205 <i>wR</i> ₂ = 0.0453	<i>R</i> ₁ = 0.0274 <i>wR</i> ₂ = 0.0557
<i>R</i> factors for all reflections	<i>R</i> ₁ = 0.0223 <i>wR</i> ₂ = 0.0458	<i>R</i> ₁ = 0.0350 <i>wR</i> ₂ = 0.0585
Residual electron density (min/max), e/Å ³	–0.945/2.221	–1.486/1.896

in the full-matrix anisotropic approximation of non-hydrogen atoms. The positions of hydrogen atoms were calculated geometrically and included into refinement in the riding model. The calculations on structure determination and refinement were performed using the SHELXTL program package [33, 34]. The main crystallographic data and results of structure refinement for compounds **I** and **II** are presented in Table 1. Selected bond lengths and angles are given in Table 2.

The coordinates of atoms, bond lengths, bond angles, and temperature parameters for the synthesized complexes were deposited with the Cambridge Crystallographic Data Centre (CIF files CCDC

nos. 1877115 (**I**) and 1876364 (**II**); deposit@ccdc.cam.ac.uk or <http://www.ccdc.cam.ac.uk>).

The thermal behavior of complexes **I** and **II** was studied by the STA method with the simultaneous detection of thermogravimetry (TG) and differential scanning calorimetry (DSC) curves. The study was conducted on an STA 449C Jupiter instrument (NETZSCH) in corundum crucibles with a cap and a hole providing a vapor pressure of 1 atm during thermolysis. The heating rate was 5°C/min to 400°C under an argon atmosphere, and the weights of the samples were 1.800–6.348 and 5.800–7.188 mg for complexes **I** and **II**, respectively. The accuracy of the temperature measurement was ±0.7°C, and the accuracy of the weight change was ±1 × 10⁻⁴ mg.

Table 2. Bond lengths (d , Å) and bond (ω , deg) and torsion (φ , deg) angles in the structures of compounds **I** and **II***

Compound I			
bond	d , Å	bond	d , Å
Bi(1)–S(1)	2.6309(10)	S(4)–C(10)	1.742(3)
Bi(1)–S(2)	2.8012(8)	N(1)–C(1)	1.327(5)
Bi(1)–S(3)	2.7335(8)	N(1)–C(2)	1.474(4)
Bi(1)–S(4)	2.6199(9)	N(1)–C(6)	1.482(5)
Bi(1)–O(1)	2.955(3)	N(2)–C(10)	1.334(4)
Bi(1)–O(1) ^a	2.961(3)	N(2)–C(11)	1.483(4)
Bi(1)–O(2)	3.007(3)	N(2)–C(15)	1.461(4)
Bi(1)–O(3) ^a	2.850(3)	O(1)–N(3)	1.265(4)
S(1)–C(1)	1.742(3)	O(2)–N(3)	1.240(4)
S(2)–C(1)	1.720(4)	O(3)–N(3)	1.250(4)
S(3)–C(10)	1.724(3)		
angle	ω , deg	angle	ω , deg
S(1)C(1)S(2)	118.1(2)	O(1) ^a Bi(1)S(4)	68.41(5)
S(1)Bi(1)S(2)	66.17(3)	O(2)Bi(1)S(1)	118.05(6)
S(3)C(10)S(4)	117.55(16)	O(2)Bi(1)S(2)	126.79(6)
S(3)Bi(1)S(4)	67.19(3)	O(2)Bi(1)S(3)	85.46(6)
S(1)Bi(1)S(3)	85.90(3)	O(2)Bi(1)S(4)	141.24(6)
S(1)Bi(1)S(4)	87.96(3)	O(3) ^a Bi(1)S(1)	166.46(7)
S(2)Bi(1)S(3)	144.16(3)	O(3) ^a Bi(1)S(2)	112.99(6)
S(2)Bi(1)S(4)	88.87(3)	O(3) ^a Bi(1)S(3)	88.86(5)
O(1)Bi(1)S(1)	77.24(6)	O(3) ^a Bi(1)S(4)	78.50(6)
O(1)Bi(1)S(2)	120.81(5)	O(1)Bi(1)O(1) ^a	148.65(9)
O(1)Bi(1)S(3)	70.28(5)	O(1)Bi(1)O(2)	42.41(8)
O(1)Bi(1)S(4)	135.73(4)	O(1)Bi(1)O(3) ^a	112.64(8)
O(1) ^a Bi(1)S(1)	130.27(6)	O(2)Bi(1)O(1) ^a	106.54(8)
O(1) ^a Bi(1)S(2)	70.10(5)	O(2)Bi(1)O(3) ^a	73.86(9)
O(1) ^a Bi(1)S(3)	119.88(5)		
angle	φ , deg	angle	φ , deg
Bi(1)S(1)S(2)C(1)	163.5(2)	S(2)C(1)N(1)C(2)	–7.2(5)
Bi(1)S(3)S(4)C(10)	–178.2(2)	S(2)C(1)N(1)C(6)	172.4(3)
S(1)Bi(1)C(1)S(2)	165.9(2)	S(3)C(10)N(2)C(11)	–0.7(4)
S(3)Bi(1)C(10)S(4)	–178.5(2)	S(3)C(10)N(2)C(15)	175.9(2)
S(1)C(1)N(1)C(2)	173.6(2)	S(4)C(10)N(2)C(11)	179.7(3)
S(1)C(1)N(1)C(6)	–6.8(5)	S(4)C(10)N(2)C(15)	–3.6(4)
Compound II			
bond	d , Å	bond	d , Å
Bi(1)–S(1)	2.6369(9)	S(3)–C(2)	1.741(4)
Bi(1)–S(2)	2.7207(9)	S(4)–C(2)	1.714(4)
Bi(1)–S(3)	2.6180(10)	N(1)–C(1)	1.322(4)
Bi(1)–S(4)	2.8290(10)	N(1)–C(3)	1.477(4)

Table 2. (Contd.)

Compound II			
bond	<i>d</i> , Å	bond	<i>d</i> , Å
Bi(1)–Cl(1)	2.9010(9)	N(1)–C(6)	1.474(4)
Bi(1)–Cl(1) ^a	3.1276(10)	N(2)–C(2)	1.316(5)
S(1)–C(1)	1.739(4)	N(2)–C(9)	1.475(5)
S(2)–C(1)	1.723(4)	N(2)–C(12)	1.468(5)
angle	ω, deg	angle	ω, deg
S(1)C(1)S(2)	117.7(2)	S(2)Bi(1)S(4)	139.61(3)
S(1)Bi(1)S(2)	67.13(3)	S(1)Bi(1)Cl(1)	150.91(3)
S(4)C(2)S(3)	118.4(2)	S(2)Bi(1)Cl(1)	84.37(3)
S(3)Bi(1)S(4)	65.90(3)	S(3)Bi(1)Cl(1)	81.54(3)
S(1)Bi(1)S(3)	89.96(3)	S(4)Bi(1)Cl(1)	116.12(3)
S(1)Bi(1)S(4)	84.76(3)	Bi(1)Cl(1)Bi(1) ^a	109.10(3)
S(2)Bi(1)S(3)	84.95(3)	Cl(1)Bi(1)Cl(1) ^a	120.83(3)
angle	φ, deg	angle	φ, deg
Bi(1)S(1)S(2)C(1)	170.7(2)	S(2)C(1)N(1)C(3)	177.6(3)
Bi(1)S(3)S(4)C(2)	–173.7(2)	S(2)C(1)N(1)C(6)	3.8(5)
S(1)Bi(1)C(1)S(2)	172.0(2)	S(3)C(2)N(2)C(9)	2.0(5)
S(3)Bi(1)C(2)S(4)	174.6(2)	S(3)C(2)N(2)C(12)	–179.1(3)
S(1)C(1)N(1)C(3)	–1.7(5)	S(4)C(2)N(2)C(9)	–178.7(3)
S(1)C(1)N(1)C(6)	–175.5(3)	S(4)C(2)N(2)C(12)	0.2(5)

* Symmetry transforms: ^a 1/2 + *x*, –*y*, *z* (I); ^a *x*, 1/2 – *y*, 1/2 + *z* (II).

RESULTS AND DISCUSSION

In the IR spectra of complexes **I** and **II**, the absorption bands in a range of 2964–2870 cm^{–1} are caused by stretching vibrations of the C–H bonds of the alkyl groups: *v*_{as}(CH₃) 2962 and 2964, *v*_s(CH₃) 2871 and 2870, and *v*_{as}(CH₂) 2930 and 2929 cm^{–1} for complexes **I** and **II**, respectively (for complex **I**, the weakly intense *v*(CH) band is observed at 2898 cm^{–1}) [35]. The high- (1149/1148 cm^{–1}) and medium-intensity (970/962 cm^{–1}) absorption bands were assigned to the *v*_{as}(CS₂) and *v*_s(CS₂) vibrations, respectively [36–38].

An important feature of the intense absorption bands at 1501 or 1493 cm^{–1} attributed to the stretching vibrations of the *v*(C–N) bond in the =NC(S)S– group is their position between the ranges of vibrations of the C=N double (1690–1640 cm^{–1}) and C–N ordinary (1360–1250 cm^{–1}) bonds [29]. This fact directly indicates the partially dual character of the C–N bond in the dithiocarbamate group. The shift of the discussed absorption bands to the high-frequency range for complexes **I** and **II** compared to the corresponding sodium dialkyl dithiocarbamates (1477/1468 cm^{–1}) indicates an increase in the contribution of double bonding to the formally ordinary N–C(S)S bond at

the covalent bonding of the dithiocarbamate (Dtc) ligands by bismuth(III).

In addition, the IR spectrum of complex **I** exhibits the nitrate group: the medium-intensity band of *v*_s(N=O) stretching vibrations at 1634 cm^{–1}, the narrow high-intensity band (1385 cm^{–1}) caused by *v*_{as}(NO₂) stretching vibrations, the medium-intensity band *v*_s(NO₂) at 1032 cm^{–1}, and the band of the planar δ(NO₃[–]) bending vibration at 714 cm^{–1} (with a shoulder at 707 cm^{–1}) [39–41]. The very significant difference (in 249 cm^{–1}) between two high-frequency bands indicates a complicated character of nitrate group coordination [39–41].

X-ray diffraction analysis was used to establish the structural organization of the obtained polymer complexes. In both complexes **I** and **II**, the unit cell includes four formula units (Figs. 1, 2). In both cases, the central bismuth atom binds two terminal Dtc ligands exhibiting the S,S'-anisobidentate coordination, where one of the Bi–S bonds (2.6199, 2.6309/2.6180, 2.6369 Å) is significantly shorter than another bond (2.7335, 2.8012/2.7207, 2.8290 Å). The coordination mode discussed leads to the formation in the complexes of two small-size four-membered

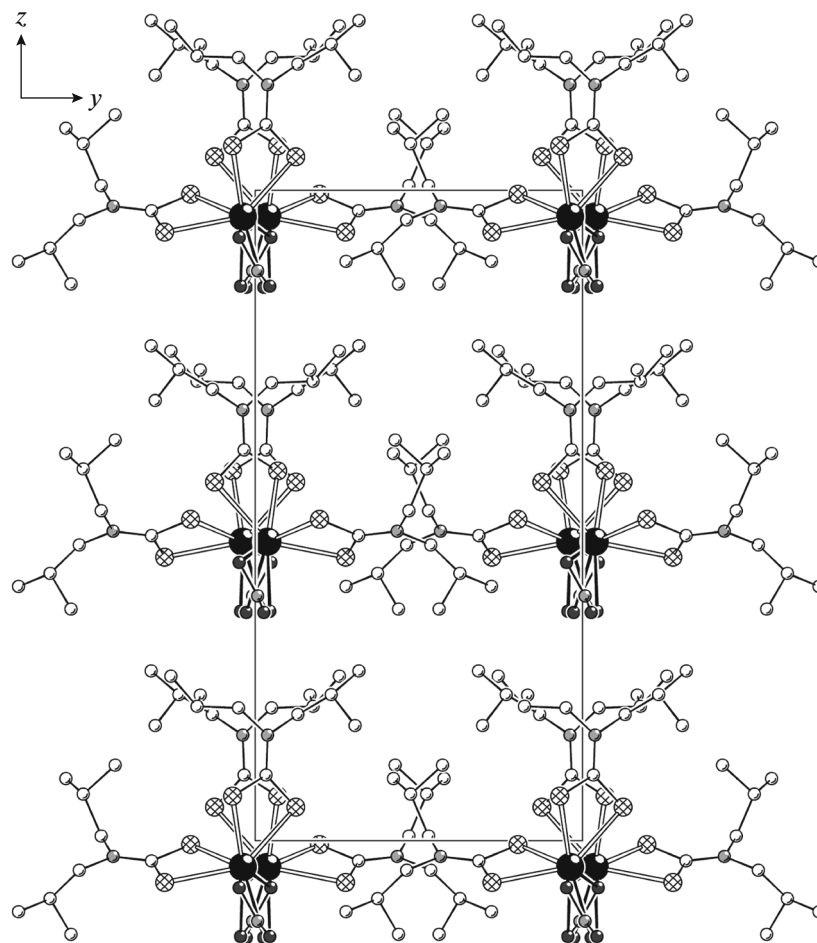


Fig. 1. Projection of the structure of compound **I** onto the yz plane. Polymer chains are directed along the x axis.

[BiS₂C] metalocycles joined by the common metal atom. The mutual arrangement of the atoms in the cycles is close to the coplanar one: the BiSSC and SBiCS torsion angles are presented in Table 2. In each complex, the most significant deviation from the planar configuration is manifested by only one metalocycle, which can be presented by its inflection along the S(1)–S(2) axis. The dihedral angle between the root-mean-square planes of the cycles in complexes **I** and **II** are 84.68° and 87.71°.

Two structural features caused by the mesomeric effect of the =NC(S)S– groups are common for the Dtc ligands in complexes **I** and **II**: (a) appreciably shorter N–C(S)S bonds (1.316–1.334 Å) compared to N–CH₂ (1.461–1.483 Å), which shows the contribution of double bonding to the formally ordinary bond, and (b) the configuration of the C₂N–CS₂ structural fragment close to the planar one, which follows from the values of the SCNC torsion angles (Table 2).

In the studied complexes, the inorganic anions NO₃[–] and Cl[–] perform the μ₂-bridging structural function joining the adjacent molecules [Bi{S₂CN(*iso*-

C₄H₉)₂}(NO₃)] and [Bi{S₂CN(C₃H₇)₂}₂Cl] into polymer chains (Figs. 3, 4). The coordination of the bridging nitrate groups is performed unusually: involving all three oxygen atoms. Therefore, the NO₃[–] groups act as double bridges: one of the oxygen atoms (O(1)) participates in binding with two adjacent Bi atoms, whereas each oxygen atom of two others, O(2) and O(3), coordinates only one of the metal atoms (Fig. 3). Therefore, on the whole, the nitrate group is involved in the bidentate coordination to each adjacent Bi atom.

Two types of the bridging coordination mode of nitrate groups have previously been described for the bismuth(III) dithiocarbamate nitrate complexes involving one (μ₂-nitrate-*O*: Bi–O(NO₂)–Bi, the Bi–O bond lengths are 2.694 and 2.725 Å [24]) or two oxygen atoms (μ₂-nitrate-*O,O'*: Bi–O(NO)O–Bi, Bi–O 2.772 and 2.827 Å [21]; Bi–O 2.723 and 2.856 Å [24]).¹ In our case, the Bi–O bonds (in a range of

¹The data for the structure of the polymer complex [Bi{S₂CN(CH₂)₅}₂(NO₃)_n] studied at 299 K [21] and 100 K [24] are presented.

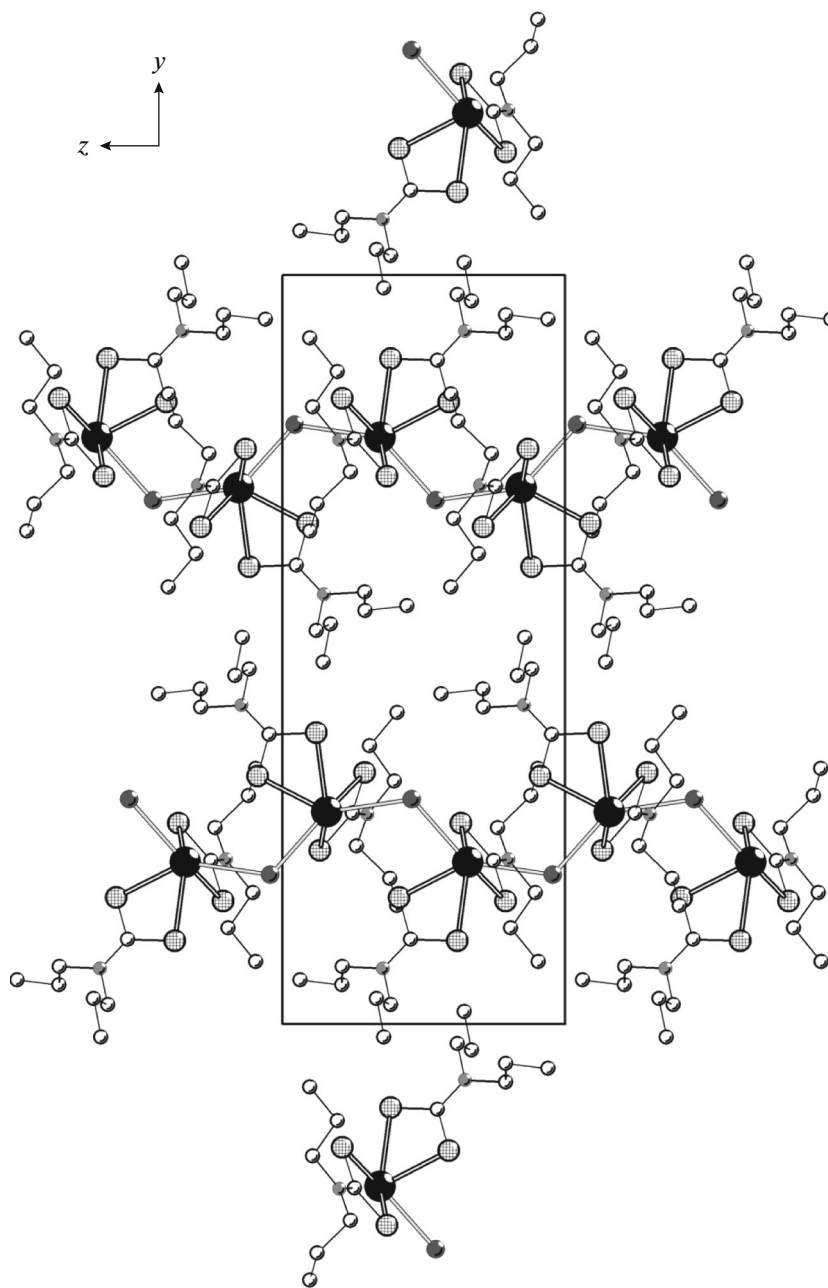


Fig. 2. Projection of the structure of compound **II** onto the yz plane. Polymer chains are directed along the z axis.

2.850–3.007 Å (Table 2)) are much longer, and the structure formation of the polymer chain in compound **I** differs basically due to a greater number of less strong Bi–O bonds (Fig. 3). Only one more compound in which the nitrate groups are involved in the same way in binding of the adjacent bismuth complexes is known: the heteroleptic complex additionally including two-charge alkoxy groups of pentaethylene glycol characterized by stronger Bi–O bonds (2.57–3.00 Å) [42]. In addition, the compounds in which the nitrate group forms four (2.621–2.903 Å) [43] or six

(2.725–2.875 Å) Bi–O bonds [44] and joins three bis-bismuth atoms are also described among the polynuclear complexes with the purely oxygen environment of the central bismuth atom.

The structural organization of complex **II** is close, to the highest extent, to that described previously for compounds $[\text{Bi}\{\text{S}_2\text{CN}(\text{CH}_2)_4\}_2\text{Cl}] \cdot \text{CHCl}_3$ [27] and $[\text{Bi}\{\text{S}_2\text{CN}(\text{C}_2\text{H}_5)(\text{C}_2\text{H}_4\text{OH})\}_2\text{Cl}]$ [28]. In all these cases, the complexes contain two nonequivalent S,S' -anisobidentate Dtc ligands and the μ_2 -bridging chlorine atom asymmetrically binding the bismuth atoms.

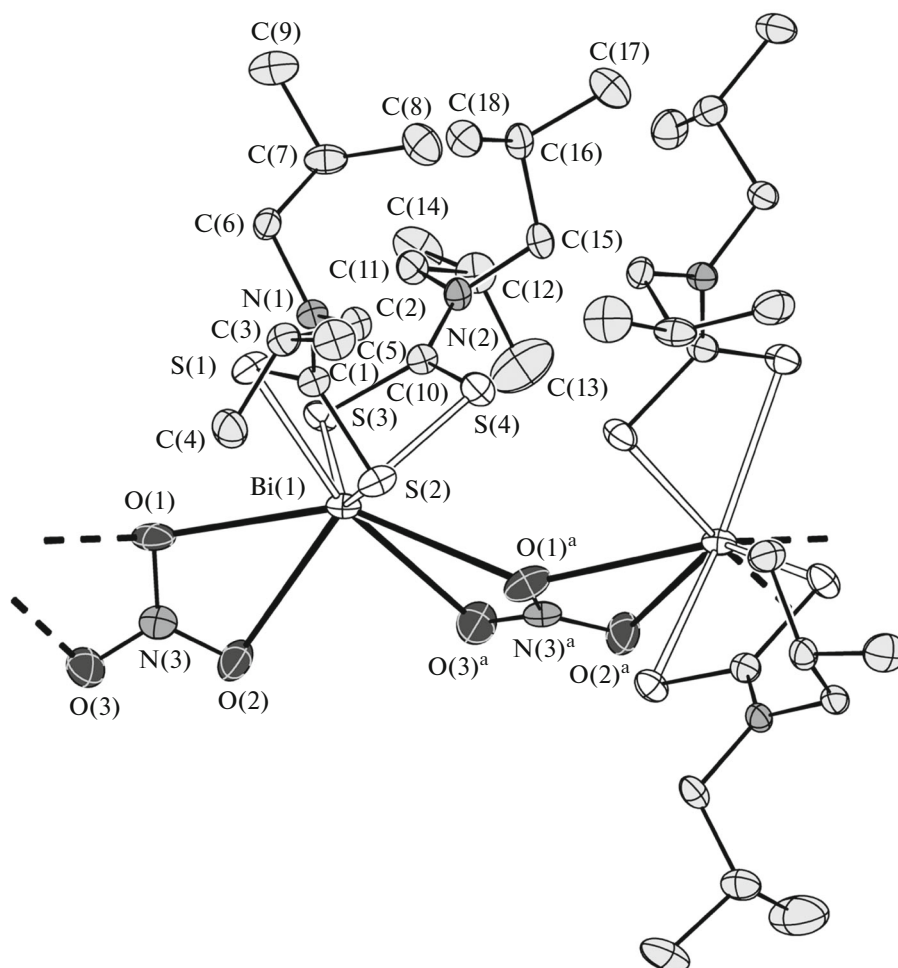


Fig. 3. Two-link fragment of the polymer chain $[\text{Bi}\{\text{S}_2\text{CN}(\text{iso-C}_4\text{H}_9)_2(\text{NO}_3)\}_n$. Ellipsoids of 50% probability; symmetry transform: ^a $1/2 + x, -y, z$. Hydrogen atoms are omitted.

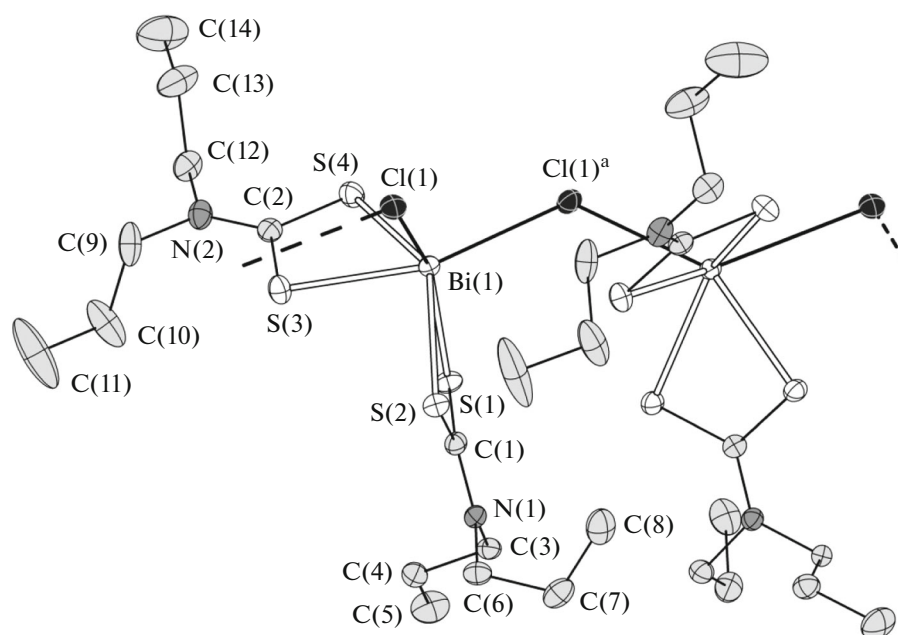


Fig. 4. Two-link fragment of the polymer chain $[\text{Bi}\{\text{S}_2\text{CN}(\text{C}_3\text{H}_7)_2\}_2\text{Cl}]_n$. Ellipsoids of 50% probability; symmetry transform: ^a $x, 1/2 - y, 1/2 + z$. Hydrogen atoms are omitted.

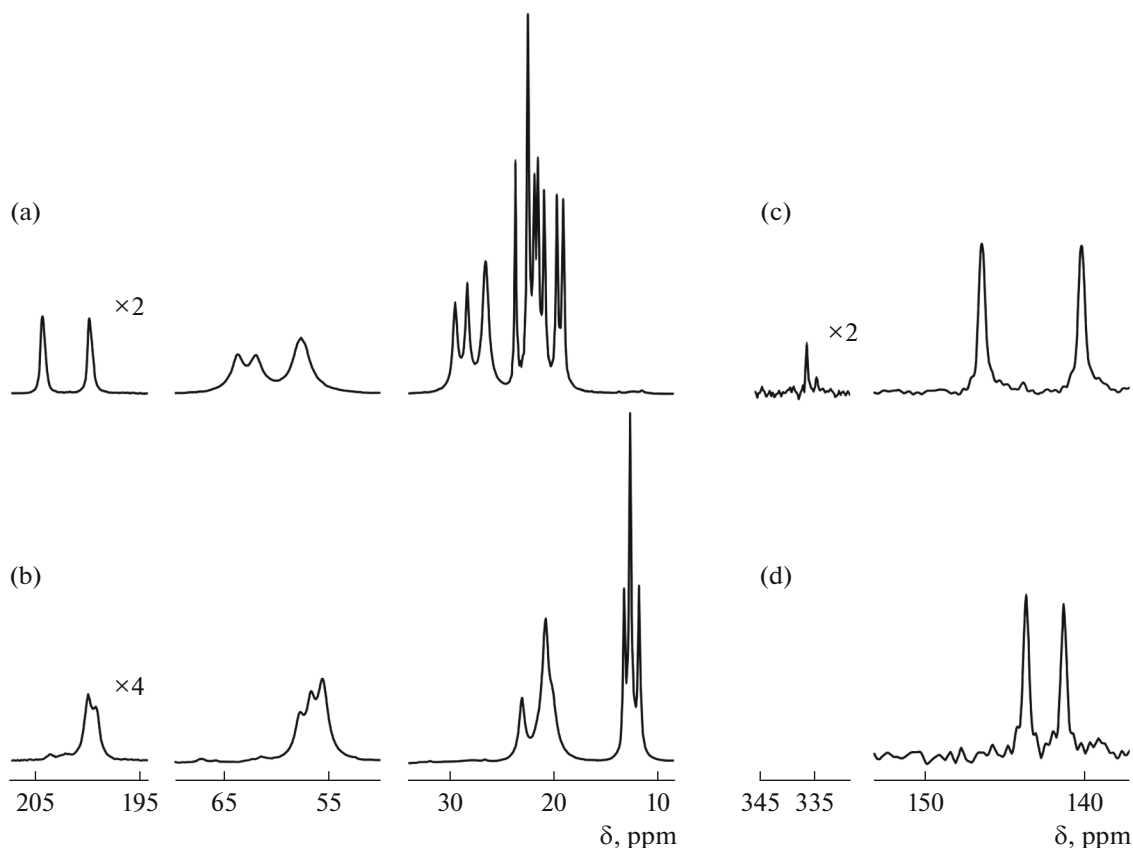


Fig. 5. (a, b) ^{13}C and (c, d) ^{15}N CP-MAS NMR spectra of the polycrystalline samples of compounds (a, c) **I** and (b, d) **II**. The number of acquisitions/rotation frequency of the samples (in Hz): (a) 23400/10000, (b) 30000/5000, (c) 31648/5000, and (d) 78200/5000.

The Bi–Cl bond lengths (2.9010 and 3.1276 Å) in the structure of compound **II** are consistent with the corresponding characteristics of μ_2 -Cl ligands also in such inorganic anions as $[\text{Bi}_2\text{Cl}_9]^{3-}$ [18], $[\text{Bi}_2\text{Cl}_{10}]^{4-}$ [45], and $[\text{Bi}_3\text{Cl}_{12}]^{3-}$ [46], as well as in polymer $([\text{BiCl}_5]^{2-})_n$ [47].

The value of the BiBiBi angle ($163.436(4)^\circ$) in the zigzag polymer chain of the structure of compound **I** shows that the chain is smoothed. In the chain of the structure of compound **II** (Fig. 4), the deviation from linearity is much more pronounced: the BiBiBi angle is $140.983(4)^\circ$. Using the overall coordination of two terminal (Dtc) and two bridging (NO_3^-) ligands in compound **I**, the central bismuth atom forms the eightfold environment $[\text{Bi}_4\text{O}_4]$. In complex **II**, the bridging chlorine atoms similarly build up the inner sphere of the metal to $[\text{Bi}_4\text{Cl}_2]$.

The ^{13}C , ^{15}N CP-MAS NMR spectra of complexes **I** and **II** indicate the individual character of the synthesized compounds (Fig. 5). The Dtc groups in the studied complexes are characterized by substantially lower ^{13}C chemical shifts compared to the initial sodium salts, which is a direct consequence of the

covalent binding of the Dtc ligands by bismuth(III). The ^{13}C NMR spectra of complexes **I/II** (Figs. 5a, 5b) containing the resonance signals of the $=\text{NC}(\text{S})\text{S}-$ (1 : 1), $=\text{NCH}_2-$ (1 : 1 : 2), $=\text{CH}-$ (1 : 1 : 2)/ $-\text{CH}_2-$ (1 : 2 : 1), and $-\text{CH}_3$ (1 : 2 : 1 : 1 : 1 : 1 : 1)/(1 : 2 : 1) groups are completely consistent with the X-ray diffraction data indicating the presence of two Dtc ligands in each complex. This shows their nonequivalence concerning both the Dtc groups directly bonded to the central bismuth atom and the structural groups in the alkyl substituents. In turn, each ^{15}N NMR spectrum is represented by two resonance signals (1 : 1) of the $=\text{NC}(\text{S})\text{S}-$ groups and the additional low intense signal of the NO_3 group in dithiocarbamato-nitrato complex **I** (Figs. 5c, 5d).

The thermal behavior of the synthesized complexes was studied in argon by the STA method with the simultaneous detection of the TG and DSC curves (Figs. 6, 7). The first indications to the mass loss onset by the samples of complexes **I** and **II** appear at 132 and 160°C , respectively, which determines the boundary of their chemical stability. The endoeffects in the DSC curves with extremes at 160.0 and 147.7°C correspond to melting of the complexes: the extrapolated melting

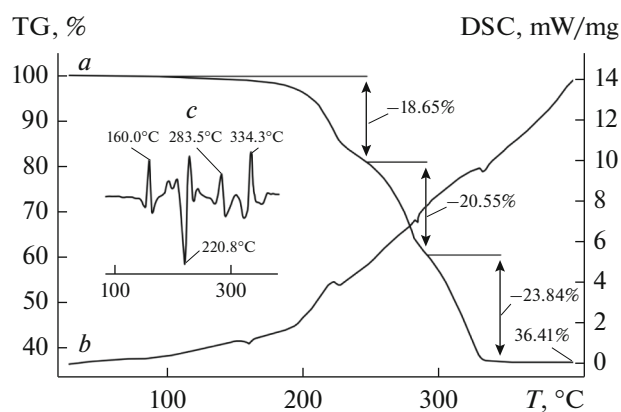


Fig. 6. (a) TG and (b) DSC curves for complex I. (c) Inset: the second derivative of the DSC curve.

points are equal to 156.2 and 145.5°C, respectively. (The following melting ranges were determined for the samples by the independent determination in a glass capillary: 155–158 and 146–148°C.) The double differentiation was performed for the DSC curves of complex I to reveal more distinctly the characteristic points of the low intense thermal effects (Fig. 6c).

The TG curve of compound I exhibits three inflection points indicating a complicated character of thermolysis. The initial region (before the first point at 246.0°C) is characterized by a mass loss of 18.65%. Since the exoeffect at 220.8°C is projected onto this region, it is reasonable to assume that the thermal destruction at the initial stage involves the NO₃ group and one of the alkyl substituents (17.37%). Thermal transformations in the range of relatively low temperatures involving NO₃ groups are fairly typical of the dithiocarbamate nitrate complexes [48]. In the subsequent regions, the complex undergoes defragmentation at the remained alkyl substituents and Dtc groups to form Bi₂S₃ (the residual weight of which equal to 36.41% is somewhat lower than the calculated weight equal to 37.82%) as the major final product of the thermal transformations of complex I. The DSC curve includes two endotherms (at 283.5 and 334.3°C) corresponding to each of thermolysis stages discussed (Fig. 6c).

The thermolysis of complex II formally proceeds via one stage (Fig. 7a). However, the differentiation of the TG curve allows one to reveal the inflection point at 236.0°C. The mass loss at the initial stage (before this point) equal to 15.92% indicates the dissociation of two –C₃H₇ groups (calcd. 14.43%). The subsequent run of the TG curve includes the region (below 301.0°C) showing the main mass loss (34.28%) and the final stage of the smooth desorption of volatile thermolysis products (6.67%), which is completed by the stabilization of the residual weight at 388.0°C (43.13%). The latter with a high accuracy corresponds to the expected weight for Bi₂S₃ (calcd. 43.06%),

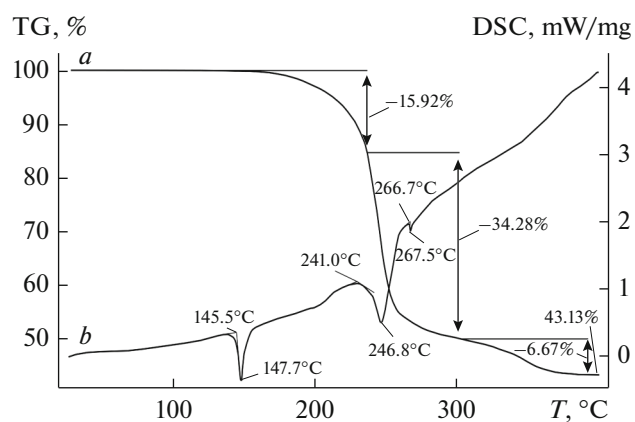


Fig. 7. (a) TG and (b) DSC curves for complex II.

which is consistent with the data on studying the thermolysis of the solvated form of the bismuth(III) dithiocarbamate-chloride of [Bi{S₂CN(CH₂)₄}₂Cl] · CHCl₃ [27]. The DSC curve exhibits the endotherms at 246.8 and 267.5°C (Fig. 7b) along with the thermal effect of melting. The first endotherm is due to the thermal decomposition of the substance (the extrapolated temperature of the process is 241.0°C). The second, narrow, and very low intense endotherm corresponds to the melting of traces of reduced bismuth (extrapolated mp = 266.7°C). Compact metallic bismuth melts at 271.442°C [49]. In our case, a decrease in the melting point can be explained by two factors: a small size of the metallic particles and the presence of Bi₂S₃ as the major component [49], whose gray-black finely dispersed powder was observed in the crucibles in both cases.

ACKNOWLEDGMENTS

The authors are grateful to F.U. Shah (Luleå University of Technology, Luleå, Sweden) for help in recording the ¹³C CP-MAS NMR spectra.

CONFLICT OF INTEREST

The authors declare that they have no conflicts of interest.

REFERENCES

1. Chauhan, H.P.S., Joshi, S., and Carpenter, J., *J. Therm. Anal. Calorim.*, 2016, vol. 124, no. 1, p. 117.
2. Tamilvanan, S., Gurumoorthy, G., Thirumaran, S., and Ciattini, S., *Polyhedron*, 2017, vol. 121, p. 70.
3. Ariza-Roldán, A.O., López-Cardoso, E.M., Rosas-Valdez, M.E., et al., *Polyhedron*, 2017, vol. 134, p. 221.
4. Tamilvanan, S., Gurumoorthy, G., Thirumaran, S., and Ciattini, S., *Polyhedron*, 2017, vol. 123, p. 111.
5. Li, H., Lai, C.S., Wu, J., et al., *J. Inorg. Biochem.*, 2007, vol. 101, no. 5, p. 809.

6. Ishak, D.H.A., Ooi, K.K., Ang, K.-P., et al., *J. Inorg. Biochem.*, 2014, vol. 130, p. 38.
7. Ozturk, I.I., Banti, C.N., Kourkoumelis, N., et al., *Polyhedron*, 2014, vol. 67, p. 89.
8. Arda, M., Ozturk, I.I., Banti, C.N., et al., *RSC Adv.*, 2016, vol. 6, p. 29026.
9. Guo, Y.-C., Ma, Q.-G., Chen, S.-Y., et al., *Chin. J. Struct. Chem.*, 2015, vol. 34, no. 7, p. 1028.
10. Venkatachalam, V., Ramalingam, K., Casellato, U., and Graziani, R., *Polyhedron*, 1997, vol. 16, no. 7, p. 1211.
11. Monteiro, O.C., Nogueira, H.I.S., Trindade, T., and Motevalli, M., *Chem. Mater.*, 2001, vol. 13, no. 6, p. 2103.
12. Lai, C.S. and Tiekink, E.R.T., *Z. Kristallogr.*, 2007, vol. 222, no. 10, p. 532.
13. Sun, R.-Z., Guo, Y.-C., Liu, W.-M., et al., *Chin. J. Struct. Chem.*, 2012, vol. 31, no. 5, p. 655.
14. Ivanov, A.V., Egorova, I.V., Ivanov, M.A., et al., *Dokl. Phys. Chem.*, 2014, vol. 454, no. 1, p. 16.
15. Sivasekar, S., Ramalingam, K., Rizzoli, C., and Alexander, N., *Inorg. Chim. Acta*, 2014, vol. 419, p. 82.
16. Chauhan, R., Chaturvedi, J., Trivedi, M., et al., *Inorg. Chim. Acta*, 2015, vol. 430, p. 168.
17. Gowda, V., Sarma, B., Laitinen, R.S., et al., *Polyhedron*, 2017, vol. 129, p. 123.
18. Ivanov, A.V., Gerasimenko, A.V., Egorova, I.V., et al., *Russ. J. Coord. Chem.*, 2018, vol. 44, no. 8, p. 518. <https://doi.org/10.1134/S1070328418080043>
19. Yin, H. and Wang, C., *Appl. Organomet. Chem.*, 2004, vol. 18, no. 4, p. 195.
20. Yin, H.D., Wang, C.H., and Ma, C.L., *Chem. Res. Chin. Univ.*, 2004, vol. 20, no. 5, p. 565.
21. Yin, H.D., Wang, C.H., and Wang, L., *Chin. J. Struct. Chem.*, 2004, vol. 23, no. 10, p. 1201.
22. Yin, H.D., Hong, M., and Wang, C.H., *Indian J. Chem., Sect. A: Inorg., Bio-Inorg., Phys., Theor. Anal. Chem.*, 2005, vol. 44, no. 7, p. 1401.
23. Li, F., Yin, H.-D., and Wang, D.-Q., *Acta Crystallogr., Sect. E: Struct. Rep. Online*, 2007, vol. 63, no. 6, p. m1577.
24. Kun, W.N., Mlowe, S., Nyamen, L.D., et al., *Chem.-Eur. J.*, 2016, vol. 22, no. 37, p. 13127.
25. Raston, C.L., Rawbottom, G.L., and White, A.H., *J. Chem. Soc., Dalton Trans.*, 1981, no. 6, p. 1352.
26. Raston, C.L., Rawbottom, G.L., and White, A.H., *J. Chem. Soc., Dalton Trans.*, 1981, no. 6, p. 1372.
27. Koh, Y.W., Lai, C.S., Du, A.Y., et al., *Chem. Mater.*, 2003, vol. 15, no. 24, p. 4544.
28. Jamaluddin, N.A., Baba, I., Halim, S.N.A., and Tiekink, E.R.T., *Z. Kristallogr. NCS*, 2015, vol. 230, no. 3, p. 239.s
29. Byr'ko, V.M. *Ditiokarbamaty* (Dithiocarbamates) Moscow: Nauka, 1984.
30. Ivanov, A.V. and Antzutkin, O.N., *Top. Curr. Chem.*, 2005, vol. 246, p. 271.
31. Pines, A., Gibby, M.G., and Waugh, J.S., *J. Chem. Phys.*, 1972, vol. 56, no. 4, p. 1776.
32. Ratcliffe, C.I., Ripmeester, J.A., and Tse, J.S., *Chem. Phys. Lett.*, 1983, vol. 99, no. 2, p. 177.
33. *APEX2 (version 1.08), SAINT (version 7.03), SADABS (version 2.11), SHELXTL (version 6.12)*, Madison: Bruker AXS Inc., 2004.
34. Sheldrick, G.M., *Acta Crystallogr., Sect. A: Found. Crystallogr.*, 2008, vol. 64, no. 1, p. 112.
35. Kazitsyna, L.A. and Kupletskaya, N.B. *Primenenie UF-, IK-, YaMR- i mass-spektroskopii v organicheskoi khimii* (Applications of UV, IR, NMR, and Mass Spectroscopy in Organic Chemistry), Moscow: Mosk. Univ., 1979.
36. Yin, H.D., Li, F., and Wang, D., *J. Coord. Chem.*, 2007, vol. 60, no. 11, p. 1133.
37. Brown, D.A., Glass, W.K., and Burke, M.A., *Spectrochim. Acta, Part A*, 1976, vol. 32, no. 1, p. 137.
38. Kellner, R., Nikolov, G.S., and Trendafilova, N., *Inorg. Chim. Acta*, 1984, vol. 84, no. 2, p. 233.
39. Tarasevich B.N., *IK spektry osnovnykh klassov organicheskikh soedinenii* (IR Spectra of Main Classes of Organic Compounds), Moscow: MGU im. M.V. Lomonosova, 2012.
40. Bellamy, L.J., *The Infrared Spectra of Complex Molecules*, New York: Wiley, 1958.
41. Nakamoto, K., *Infrared Spectra and Raman Spectra of Inorganic and Coordination Compounds*, New York: Wiley, 1986.
42. Rogers, R.D., Bond, A.H., and Aguinaga, S., *J. Am. Chem. Soc.*, 1992, vol. 114, no. 8, p. 2960.
43. Feyand, M., Koppen, M., Friedrichs, G., and Stock, N., *Chem.-Eur. J.*, 2013, vol. 19, no. 37, p. 12537.
44. Senevirathna, D.C., Werrett, M.V., Blair, V.L., et al., *Chem.-Eur. J.*, 2018, vol. 24, no. 26, p. 6722.
45. Adonin, S.A., Gorokh, I.D., Samsonenko, D.G., et al., *Russ. J. Coord. Chem.*, 2016, vol. 42, no. 11, p. 695. <https://doi.org/10.1134/S1070328416110014>
46. Zaeva, A.S., Ivanov, A.V., Gerasimenko, A.V., and Sergienko, V.I., *Russ. J. Inorg. Chem.*, 2015, vol. 60, no. 2, p. 203. <https://doi.org/10.1134/S0036023615020229>
47. Adonin, S.A., Samsonenko, D.G., Sokolov, M.N., and Fedin, V.P., *Russ. J. Coord. Chem.*, 2016, vol. 42, no. 1, p. 27. <https://doi.org/10.1134/S1070328416010012>
48. Loseva, O.V., Rodina, T.A., Ivanov, A.V., et al., *Russ. Chem. Bull., Int. Ed.*, 2019, vol. 68, no. 4, p. 782. <https://doi.org/10.1007/s11172-019-2486-3>
49. Lin, J.-C., Sharma, R.C., and Chang, Y.A., *J. Phase Equilib.*, 1996, vol. 17, no. 2, p. 132.

Translated by E. Yablonskaya